HHS Public Access

Author manuscript

Polym Chem. Author manuscript; available in PMC 2016 March 07.

Published in final edited form as:

Polym Chem. 2015 March 7; 6(9): 1465–1473. doi:10.1039/C4PY01503G.

Synthetic Strategy for Preparing Chiral Double-semicrystalline Polyether Block Copolymers

Alaina J. McGrath[a], **Weichao Shi**[a], **Christina G. Rodriguez**[a], **Edward J. Kramer**[a,b,c], **Craig J. Hawker**[a,b,d], and **Nathaniel A. Lynd**[a]

Craig J. Hawker: hawker@mrl.ucsb.edu; Nathaniel A. Lynd: lynd@mrl.ucsb.edu

[a]Materials Research Laboratory, University of California, Santa Barbara, CA 93106, USA

[b]Materials Department, University of California, Santa Barbara, CA 93106, USA

[c]Department of Chemical Engineering, University of California, Santa Barbara, CA 93106, USA

[d]Department of Chemistry and Biochemistry, University of California, Santa Barbara, CA 93106, USA

Abstract

We report an effective strategy for the synthesis of semi-crystalline block copolyethers with well-defined architecture and stereochemistry. As an exemplary system, triblock copolymers containing either atactic (racemic) or isotactic (*R* or *S*) poly(propylene oxide) end blocks with a central poly(ethylene oxide) mid-block were prepared by anionic ring-opening procedures. Stereochemical control was achieved by an initial hydrolytic kinetic resolution of racemic terminal epoxides followed by anionic ring-opening polymerization of the enantiopure monomer feedstock. The resultant triblock copolymers were highly isotactic (meso triads [*mm*]% ~ 90%) with optical microscopy, differential scanning calorimetry, wide angle x-ray scattering and small angle x-ray scattering being used to probe the impact of the isotacticity on the resultant polymer and hydrogel properties.

Introduction

Polyether based block copolymers are a versatile and commercially important class of materials with poly(ethylene oxide) (PEO) being the prototypical polyether used for biomedical applications due to its water-solubility and biocompatibility.[1] These properties allow PEO to have utility in a wide range of products from personal care items[2] to pharmaceuticals.[1, 3] The function of PEO-based polymers can be further modified by incorporation of hydrophobic blocks, such as poly(propylene oxide) (PPO), where the introduction of hydrophobicity can impart LCST-type phase behavior, micellar self-assembly, and hydrogelation.[4–6] Block copolymers consisting of PEO and PPO domains, a sub-set of which are the widely studied pluronics®, have proved to be useful for the delivery

Correspondence to: Craig J. Hawker, hawker@mrl.ucsb.edu; Nathaniel A. Lynd, lynd@mrl.ucsb.edu.

Electronic Supplementary Information (ESI) available: experimental setup, ^{1}H NMR, and additional GPC traces and SAXS data. See DOI: 10.1039/b000000x/

of small molecule and DNA based therapeutics,[7, 8] as scaffolds for cell and tissue growth,[9, 10] and as coverings for burn wounds.[11, 12] The available strategies for assembly and encapsulation can further be expanded by the inclusion of ionic and functional motifs which has in turn expanded the potential applications of PEO-based polymers.[13–18] Within the context of industrially important polyether-based block copolymers, such as PEO-*b*-PPO, isotacticity has not yet been explored. Likewise, synthetic concepts for introducing isotacticity into polyether-based block polymers have not been reported.

The catalyst-driven polymerization of racemic propylene oxide (PO) to prepare stereoregular PPO homopolymers has been widely studied in the literature, beginning with the seminal work of Pruitt and Bagget in 1955.[19] However, these polymerizations typically resulted in enriched, and not fully isotactic PPO.[20–24] More recently, Co^{III} complexes developed in the Coates group have allowed a variety of racemic epoxides to be polymerized in a stereoregular fashion to produce highly isotactic polyethers.[25–28] To our knowledge, the synthesis of a stereoregular polyether-based block copolymer has only been reported once in the literature; the preparation of *it*-poly(propylene oxide)-*b*-poly(phenylene ethynylene) was achieved by post-polymerization coupling of the two blocks together.[29] Therefore, the ability to develop a synthetic platform to synthesize well-defined block copolymers containing isotactic polyethers is advantageous.

Herein, we combine the hydrolytic kinetic resolution of terminal epoxides with the advantages of anionic ring-opening polymerization to produce well-defined triblock copolymers with *it*-PPO end blocks.[30] The influence of both semi-crystalline blocks was explored by x-ray scattering (both wide angle (WAXS) and small angle (SAXS)), optical microscopy and differential scanning calorimetry (DSC). Significantly, tacticity was shown to influence a variety of properties for both the block copolymers as well as the resulting hydrogels.

Results and Discussion

Materials

Propylene oxide (PO, TCI, >99%), and (*S*,*S*)- and (*R*,*R*)-(+)-*N*,*N*′-Bis(3,5-di-*tert*-butylsalicylidene)-1,2-cyclohexanediaminocobalt(II) ((*S*,*S*)- or (*R*,*R*)-(salen)Co^{II}), (Sigma Aldrich) were used as received. Anhydrous THF and toluene were obtained from a JC Meyer solvent system. All other reagents were purchased from commercial sources and used as received unless specified. Poly(ethylene oxide) (PEO) (Sigma Aldrich, M_n = 10,000 and 20,000 g/mol) was dried by azeotropic removal of water with toluene. Kinetically resolved propylene oxide monomers were degassed by several freeze-pump-thaw cycles and distilled from CaH_2. Potassium naphthalenide was prepared from the addition of potassium metal (3.0 g, 77 mmol) to recrystallized naphthalene (10 g, 78 mmol) in anhydrous THF (250 mL, 0.3 M) under argon. The reaction, equipped with a glass-coated stirbar, was allowed to stir overnight at room temperature before use. All air and moisture sensitive reactions were carried out using standard Schlenk-line techniques.

Instrumentation

^{1}H and ^{13}C NMR spectroscopy were performed on a Bruker Avance DMX 500 MHz or Varian VNMRS 600 MHz spectrometer at room temperature and referenced to the residual non-deuterated or deuterated solvent shift of $CDCl_3$ (7.26 ppm and 77.16 ppm respectively). Gel permeation chromatography (GPC) was carried out on a Waters chromatograph equipped with a Waters Alliance HPLC system pump (2690 separation module) and two Agilent columns (PLGEL 5 μm, and MIXED-D 300 × 7.5 mm). Detection was provided by a Waters 2410 differential refractometer and $CHCl_3$ with 1% TEA was used as the mobile phase. Chromatograms were run at room temperature and calibrated to PEO standards. Optical rotation measurements were conducted on a Rudolph Research Analytical Autopol III polarimeter with a sodium lamp (λ = 489 nm) at 23°C and are reported as $[\alpha]^{T(°C)}\ \lambda\ (c)$.

Representative Procedure for Kinetic Resolution of Propylene Oxide Monomers

(*R*) and (*S*)-PO were synthesized according to the literature procedure,[31] which was modified slightly to accommodate large scale reactions.

(*S*)-PO—In a round bottom flask, glacial acetic acid (36.1 mmol, 2.07 mL) was added to a solution of *S*,*S*-(salen)Co^{II} (3.44 mmol, 2.08 g, 0.002 equiv) in toluene (43 mL, 0.08 M) and allowed to stir at room temperature in air for 30 min. During this time the reaction changed from red-orange to brown. The active catalyst was then concentrated in vacuo, leaving a brown solid, which was re-dissolved in propylene oxide (PO) (1.72 mol, 120 mL) and cooled to 0 °C. The round bottom flask was equipped with a reflux condenser and distilled water (946 mmol, 17.0 mL, 0.55 equiv) was added to the reaction dropwise. Special precaution was taken to add the water very slowly to keep the exotherm under control. The reaction was allowed to warm to room temperature and was stirred overnight. The reaction conversion was checked by ^{1}H NMR and (*S*)-PO was isolated by distillation (45 g, 45%). $[\alpha]^{23}_{D}$ −11.7°(neat); lit. $[\alpha]^{23}_{D}$ −11.6°(neat).[31]

(*R*)-PO—was prepared using an analogous procedure with *R*,*R*-(salen)Co^{II} as the catalyst. $[\alpha]^{23}_{D}$ +11.1°(neat); lit. $[\alpha]^{25}_{D}$ +11.2°(neat).[32]

General Procedure for Synthesis of PPO-*b*-PEO-*b*-PPO Triblock Copolymers

All polymerizations were performed in custom thick-walled glass reactors fitted with ACE-threads. The reactors were equipped with glass coated stirbars, connected to a Schlenk line, and fitted with Teflon stoppers and custom burets containing anhydrous THF and PO (see supporting information, Figure S1 for experimental setup). Reactors were assembled hot, cooled under vacuum, and charged with telechelic PEO and 18-crown-6 (18C6, 2 equiv per chain end) under argon. Anhydrous toluene was added to the reactor via syringe, stirred at 50 °C for 10–20 minutes, and removed under vacuum to help eliminate water by azeotrope. The reactor was then submitted to several cycles of evacuation followed by argon purge to remove oxygen from the system. THF was added to the reactor via buret until PEO was completely dissolved. Heating to 40 °C was necessary for all solids to go into solution. The potassium alkoxide macroinitiator was formed by titration of PEO with potassium naphthalenide solution (3 M in THF) until the green color persisted, indicating complete deprotonation with the potassium naphthalenide solution being added via cannula through a

6 mm puresep septum. PO monomer was added to the reactor all at once via buret at room temperature, which immediately quenched the green color, turning pink and then pale yellow. Polymerizations were carried out at room temperature for 7–11 days or until no appreciable change in molecular weight was observed by GPC. Reactions were quenched with HCl-treated methanol and solvent was removed under reduced pressure. The crude reaction mixture was then re-dissolved in DCM, extracted with 10% $NaHSO_4$ aqueous solution, washed with brine, dried with $MgSO_4$ and concentrated in vacuo. The polymer was purified by a short silica plug using acetone as the eluent to remove a small amount of low molecular weight impurity and switching to 20% MeOH/DCM to elute the desired triblock copolymer. M_w of PPO was determined by 1H NMR (see supporting information, Figure S2). Dispersities were determined by GPC calibrated with PEO standards and [*mm*] (%) was determined by the *mm* triad content in the ^{13}C NMR.[33]

***it*-(*S*)-PPO-*b*-PEO-*b*-*it*-(*S*)-PPO—**M_n = 28,600 g/mol (30 wt% PPO, 70 wt% PEO); Đ = 1.26; [*mm*] = 90%; ^1H NMR ($CDCl_3$, 600 MHz) δ 3.50 (s, 12 H, PEO –CH_2), 3.42−3.38 (m, 2 H, PPO –CH_2), 3.28−3.27 (m, 1 H, PPO –C*H*), 0.99 (d, *J* = 4.8 Hz, 3 H, PPO –CH_3). ^{13}C NMR ($CDCl_3$, 150 MHz) δ 75.20 (PPO –*C*H, *mm*), 73.12 (PPO –*C*H_2, *m*), 70.30 (PEO –*C*H_2), 17.19 (PPO – *C*H_3).

***at*-PPO-*b*-PEO-*b*-*at*-PPO—**M_n = 28,600 g/mol (30 wt% PPO, 70 wt% PEO); Đ = 1.27; [*mm*] = 25%; ^1H NMR ($CDCl_3$, 600 MHz) δ 3.63 (s, 12 H, PEO –CH_2), 3.58−3.48 (m, 2 H, PPO – CH_2), 3.41−3.37 (m, 1 H, PPO –C*H*), 1.14−1.12 (m, 3 H, PPO – CH_3). ^{13}C NMR ($CDCl_3$, 150 MHz) δ 75.42 (PPO –*C*H, *mm*), 75.26 (PPO –*C*H, *mr* + *rm*), 75.23 (PPO –*C*H, *mr* + *rm*), 75.03 (PPO –*C*H, *rr*), 73.27 (PPO –*C*H_2, *m*), 72.83 (PPO –*C*H_2, *rrm* or *mrr*), 70.49 (PEO –*C*H_2), 17.27 (PPO –*C*H_3).

***it*-(*R*)-PPO-*b*-PEO-*b*-*it*-(*R*)-PPO—**M_n = 28,800 g/mol (31 wt% PPO, 69 wt% PEO); Đ = 1.36; [*mm*] = 93%

***it*-(*S*)-PPO-*b*-PEO-*b*-*it*-(*S*)-PPO—**M_n = 14,000 g/mol (29 wt% PPO, 71 wt% PEO); Đ = 1.08; [*mm*] = 90%

***it*-(*R*)-PPO-*b*-PEO-*b*-*it*-(*R*)-PPO—**M_n = 22,000 g/mol (55 wt% PPO, 45 wt% PEO); Đ = 1.17; [*mm*] = 90%

Synthesis of *it*-(*R*)-PPO Homopolymer

it-(*R*)-PPO was synthesized by trialkylaluminum-activated copolymerization of (*R*)-PO with a small incorporation of epichlorohydrin (ECH, 5 mol%) using trioctylammonium bromide as the initiator, as reported in the literature.[34, 35]

***it*-(*R*)-PPO—**M_n = 3,300 g/mol; Đ = 1.20; ^1H NMR ($CDCl_3$, 600 MHz) δ 3.59−3.49 (m, 2 H, –CH_2), 3.43−3.39 (m, 1 H, –CH), 1.13 (d, J = 6.1 Hz, 3 H, –CH_3). ^{13}C NMR ($CDCl_3$, 150 MHz) δ 75.70 (–CH, *mm*), 73.58 (–CH_2, *m*), 17.60 (–CH_3). it-(R)-PPO-co-ECH is referred to as a homopolymer due to the minimal incorporation of ECH.

Optical Microscopy

Polarized optical microscopy was employed to observe the spherulitic structures at room temperature after the samples were hot-pressed and annealed for 5 min at 100 °C. The Nikon (Japan) optical microscope was equipped with a Nikon (CoolPix P5000) camera and the wave vector direction of the polarizer was kept perpendicular to the analyzer.

Wide Angle X-ray Scattering (WAXS)

WAXS experiments were carried out on one of two instruments. The first employed an in-house x-ray generator with a rotating Cu target (data presented in Figure 4). The wavelength of the beam was 0.154 nm and a 2D position sensitive detector was placed perpendicular to the beam direction. The sample to detector distance was 245.5 mm, which afforded a scattering wavevector (q) ranging from 4 to 20 nm^{-1}. The calibration was based on Si powder with a featured peak position at 28.443°. The second instrument was a Rigaku Smartlab Diffractometer operating at a wavelength of 0.154 nm (data presented in Figure 8).

Differential Scanning Calorimetry (DSC)

Thermograms were recorded on a TA Instruments Q-2000 DSC. The rate of heating and cooling was 10 °C/min over a temperature range of −20 to 100 °C. The melting temperatures (T_m) were reported as the endothermic peak maximums.

Small Angle X-ray Scattering (SAXS)

SAXS experiments were carried out using the Advanced Light Source synchrotron at beamline 7.3.3 at Lawrence Berkeley National Laboratory. The x-ray wavelength of the beam was 0.154 nm. The thermal treatment for the sample began with heating to 130 °C which is above the order-disorder transition. Data collection began upon cooling to 40 °C in increments of 10 or 20 °C, and then heating back to 100 °C, again collecting data upon increasing temperature in increments of 10 or 20 °C. Samples were annealed at temperature for 10 minutes, and observed until the raw 2D scattering patterns appeared to remain static. Using the Nika program implemented in Igor Pro, the 2D scattering patterns were azimuthally integrated into intensity (I) versus q(nm^{-1}).[36]

Hydrogel Formation and Characterization

Films (1 mm) of *at*-PPO-*b*-PEO-*b*-*at*-PPO and *it-(S)*-PPO-*b*-PEO-*b*-*it-(S)*-PPO were hot-pressed at 70 °C and cooled slowly to room temperature. 0.106 g of pressed *it-(S)*-PPO-*b*-PEO-*b*-*it-(S)*-PPO film was placed in 0.520 g of distilled water. 0.150 g of pressed *at*-PPO-*b*-PEO-*b*-*at*-PPO film was placed in 0.653 g of distilled water. Both samples were allowed to equilibrate for 48 hours in water resulting in hydrogels of 16.9 and 18.7 polymer wt%, respectively. The samples were characterized by laboratory x-ray diffraction using a Rigaku Smartlab diffractometer with Cu Kα radiation (λ = 1.544 Å) from a scattering angle of 2.75 to 40°. The one-dimensional data was converted to scattering vector q(nm^{-1}).

Results and Discussion

To address the lack of synthetic methods to synthesize well-defined block polymers containing isotactic polyethers, we combined two well established procedures. First,

hydrolytic kinetic resolution of PO (Scheme 1A)[31] was scaled up to desirable monomer quantities (50–100 g). Extra precaution was taken to add water slowly to the reaction mixture, as well as equipping the flask with a reflux condenser, to minimize evaporation of volatile PO. Significantly, isolation of PO from the ring-opened byproduct by distillation, and the subsequent degassing and drying steps were amenable to large scale synthesis (ca. molar scale) with the optical purity of the unreacted epoxide being extremely high (>99%) when compared to literature values.[31, 32]

The ability to prepare large amounts of optically pure epoxy monomers then allowed anionic ring-opening polymerization to be exploited for the controlled synthesis of block copolymers and chain end functionalized materials.[37] While the polymerization of ethylene oxide (EO) is well-behaved under anionic conditions, the polymerization of PO is susceptible to chain-transfer reactions resulting in increased molecular weight distribution and slower polymerization kinetics. To partially address this challenge, 18-crown-6 (18C6) was added to PO polymerizations initiated by potassium salts, increasing the rate of polymerization[38] and suppressing transfer reactions.[39] Therefore, two equivalents of 18C6 per chain end of PEO macroinitiator was added to all PO polymerizations leading to negligible chain transfer and the absence of terminal alkenes in the ^{1}H NMR spectra of the resultant polymers. Scheme 1B summarizes the reaction conditions used to prepare PPO-*b*-PEO-*b*-PPO triblock copolymers.

Full characterization of the block copolymers was achieved by a combination of spectroscopic and chromatographic techniques. Due to unique signals for the EO and PO repeat units, ^{1}H and ^{13}C NMR clearly demonstrated the presence of both blocks with ^{1}H NMR being used to determine the total M_n of PPO based on the molecular weight of the starting PEO macroinitiator (see supporting information, Figure S2). Comparison of the gel permeation chromatography (GPC) trace for the starting PEO macroinitiator to corresponding *it*-PPO-*b*-PEO-*b*-*it*-PPO triblock copolymer also shows the expected increase in molecular weight and retention of low dispersity (Figure 1 and supporting information, S3) with similar results for all PEO macroinitiators studied (Table 1).

Tacticity of the PPO blocks was determined by integration of the individual peaks for the CH carbon of the propylene repeat units by ^{13}C NMR spectrum (Table 1).[33,40] The major *mm* triad and observed minor amounts of *mr*, *rm*, and *rr* triads, indicates the successful synthesis of highly tactic block copolymers (Figure 2). It should be noted that the % *mm* triad was not as high as expected based on the optical rotation measurements of the PO monomers which we attribute to small quantities of head-to-head or tail-to-tail reactions leading to inversion of the stereochemistry and an increase in the relative percentage of *mr*, *rm*, and *rr* triads.[33]

The successful synthesis of isotactic PO blocks is further supported by studying the crystal structure of the *it*-PPO homopolymer and comparison of this control sample with the corresponding double-semicrystalline triblock copolymers (both PEO and PPO domains are potentially crystalline). In traditional systems based on a single crystallizable domain, block copolymers grow into macroscopic spherulites upon supercooling from the melt. For example, the starting PEO homopolymer displays spherulites that have a regular shape and

present a Maltese cross under polarized optical light (Figure 3a). In comparison, the control *it*-PPO homopolymer shows additional undulating, concentric bright and dark bands, which is characteristic of banded spherulites (Figure 3b). This phenomenon is often found in other crystalline materials with or without molecular chirality, such as poly(L-lactide), poly[(*R*)-3-hydroxyvalerate],[41] poly(ethylene adipate)[42] and others.[43] Although molecular chirality may lead to the twisting of the crystal lamellae, it should be noted that this is not a prerequisite for lamellar twisting or spherulitic banding. Significantly, when these semi-crystalline starting materials are combined into a triblock copolymer structure with a central PEO chain tethered to two PPO end-blocks, the observed spherulitic structures are not regular (Figure 3c and d). It is proposed that this irregularity is primarily due to nanoscale confinement with lateral crystallization within lamellar layers resulting from microphase separation of the block copolymer structure.

The unique nature of these triblock copolymers, where two semi-crystalline polymers are covalently linked, should lead to two distinct crystal structures being observed in scattering patterns measured by WAXS. Comparison between the WAXS patterns for the dual semi-crystalline *it*-(*R*)-PPO-*b*-PEO-*b*-*it*-(*R*)-PPO, with the homopolymer PEO and *it*-PPO control samples and the corresponding atactic *at*-PPO-*b*-PEO-*b*-*at*-PPO triblock copolymer are presented in Figure 4. As expected, the PEO homopolymer crystallized into a monoclinic lattice[44] with characteristic peaks for the (120) plane at 13.6 nm^{-1}, and overlapping planes ((004), ($\bar{1}$24), (112), ($\bar{2}$04), (032), (014), ($\bar{1}$32) and ($\bar{2}$12)) at *ca.* 16.5 nm^{-1} (Figure 4d). In contrast, the corresponding *it*-PPO homopolymer crystallized into an orthorhombic lattice[22] which exhibited two strong reflections: (200) at 12.0 nm^{-1} and (110) at 14.8 nm^{-1} (Figure 4c). Significantly, the atactic triblock copolymer showed only broad peaks consistent with crystalline PEO domains (Figure 4b) while the isotactic triblock copolymer displayed peaks resulting from PEO and PPO crystalline domains (Figure 4a). These prominent peaks indicate dramatically different behavior for both triblock copolymer samples and clearly demonstrate that the crystal structures present in the isotactic copolymer are the same as for the corresponding homopolymers.

To further investigate the influence of multiple semi-crystalline domains and nanoscale confinement in triblock copolymer systems, DSC was used to investigate the thermal properties of *it*-PPO-*b*-PEO-*b*-*it*-PPO. The thermogram for *it*-PPO-*b*-PEO-*b*-*it*-PPO exhibited a distinct crystallization event at 13 °C (Figure 5a), separate from the crystallization of PEO (58 °C) (Figure 5a/c). Presumably, the former indicates formation of *it*-PPO crystals which corresponds roughly to the crystallization temperature of *it*-PPO homopolymer (26 °C, Figure 5d). To confirm that the new crystallization event is due to the *it*-PPO blocks, we performed the same experiment with *at*-PPO-*b*-PEO-*b*-*at*-PPO of similar molecular weight (Figure 5b) which shows a single crystallization event for the PEO mid-block domain (Figure 5b/c). As expected, the melting of *it*-PPO crystals in the triblock copolymer cannot be observed separately from the melting transition of the PEO crystals. This is due to the fact that their melting temperature ranges overlap (Figure 5c/d). Combining the observation of reduced crystallization temperature and recrystallization behavior near the melting point (Figure 5d), we conclude that the crystallization of *it*-PPO is a nucleation controlled process in both the homopolymer and triblock systems.

Synchrotron SAXS experiments were then carried out to complement the DSC study and to better understand the thermal and morphological behavior of the triblock copolymers. Above 130 °C, the atactic derivative, *at*-PPO-*b*-PEO-*b*-*at*-PPO was in the disordered state as indicated by a weak, broad peak in the scattering curve (Figure 6). This peak originates from thermal fluctuations within molecular chains, and the molecular connectivity associated with the block polymer architecture.[45, 46] Below 130 °C, microphase separation occurs leading to self-assembly of PPO and PEO blocks into ordered microphase-separated domains. The observed ratio of peak positions: 1 q*: 2 q*: 4 q* indicates that the block copolymer assembles into alternating PPO and PEO lamellae. Interestingly, the 3rd order reflection was absent from the scattering pattern, which is consistent with the volume fraction of one component being approximately 1/3 (this qualitatively corresponds to the PPO weight fraction determined by ^{1}H NMR spectroscopy, 30%) (see also supporting information, Figure S6). Subsequent to microphase separation, PEO crystallized below 46°C. During this process, the PEO chains fold back and forth and arrange into crystalline lamellae. These folded PEO chains form a helical structure on the atomic level and occupy monoclinic lattice space.[44] When PEO crystallizes, it swells the original microphase-separated domains and destroys any long range order. Therefore, after crystallization, only broad peaks shifted towards significantly lower values are observed by SAXS.

On comparison of the isotactic triblock copolymer, *it*-(*R*)-PPO-*b*-PEO-*b*-*it*-(*R*)-PPO, with the atactic derivative, *at*-PPO-*b*-PEO-*b*-*at*-PPO, of the same composition, very similar phase behavior is observed during thermal treatment (supporting information, Figure S5). Given the different crystallization behavior, this observation implies that tacticity of the PO domains does not significantly change the microphase separation behavior (order-disorder transition temperature and assembled structure) of the corresponding triblocks. To directly compare the temperature-dependence of the morphological behavior of the atactic and isotactic triblock copolymers, we plotted the domain spacing as a function of temperature for both derivatives (supporting information, Figure S7). The trends in domain spacing demonstrated that the thermal responses of the two triblock copolymers are similar: the domain spacing increased slowly as the temperature was decreased due to the increasing repulsive interactions between the PPO and PEO blocks. Ultimately, the crystallization of the PEO blocks results in a dramatic increase in domain spacing below 46 °C (Figure S7). These studies suggest that tacticity in the PPO blocks does not influence the overall thermal and morphological behaviors of the corresponding triblock in the temperature range investigated and the morphology at 40 °C is dominated by PEO crystallization. Detailed phase transitions and structural analysis will be reported in a subsequent publication. Additionally, we will report the thermal behavior and morphologies of *it*-(*R*)-PPO-*b*-PEO-*b*-*it*-(*R*)-PPO and *at*-PPO-*b*-PEO-*b*-*at*-PPO at temperatures below 40 °C.

Having established the existence of concurrent microphase separation and crystallization, we explored the potential for these dual, semi-crystalline triblock copolymers to form physical hydrogels through a combination of hydrophobic interactions and semi-crystalline crosslinks. For initial studies, 1 mm thick films of *at*-PPO-*b*-PEO-*b*-*at*-PPO and *it*-*(S)*-PPO-*b*-PEO-*b*-*it*-*(S)*-PPO were hot-pressed at 70 °C and cooled slowly to room temperature. The films were then placed in distilled water at 18.7 and 16.9 polymer wt% respectively, and left

to swell in water over the course of 48 hours. Interestingly, the hydrogel based on the isotactic triblock copolymer, *it-(S)*-PPO-*b*-PEO-*b*-*it-(S)*-PPO, retained its original film shape during water absorption, while the atactic material underwent brittle fracturing. The hydrogel prepared from the isotactic triblock was then further examined for the presence of semi-crystalline crosslinks using WAXS (Figure 7). Significantly, scattering maxima consistent with the formation of *it*-(*S*)-PPO crystallites were observed in the *it-(S)*-PPO-*b*-PEO-*b*-*it-(S)*-PPO based hydrogel (no scattering from PEO derived crystallites was observed), while a fully amorphous material was observed for the *at*-PPO-*b*-PEO-*b*-*at*-PPO hydrogel. These results demonstrate the ability to tune hydrogel properties through the synthetic design of semi-crystalline polyether-based hydrogels[47] and points the way to the design and characterization of assemblies of more complex architectures.[48]

Conclusions

A practical strategy for preparing PPO-*b*-PEO-*b*-PPO block copolymers with tacticity control has been achieved by initial kinetic resolution of epoxide monomers, followed by ring-opening anionic polymerization of the enantiopure monomer from telechelic PEO starting homopolymers. The influence of the tacticity of the PPO domains on the overall property of the triblock copolymer was significant. DSC and WAXS studies revealed the independent crystallization of the *it*-PPO and PEO blocks, consistent with dual-crystalline domains. This new synthetic concept for introducing controlled tacticity into polyether block copolymers has potential significance in both biomedical and material applications.

Supplementary Material

Refer to Web version on PubMed Central for supplementary material.

Acknowledgments

This work was supported by the MRSEC Program of the National Science Foundation under Award No. DMR 1121053 (W.S., C.G.R., E.J.K., C.J.H.). This work was partially supported by the National Institutes of Health as a Program of Excellence in Nanotechnology (HHSN268201000046C) (A.J.M., C.J.H., and N.A.L.). Beamline 7.3.3 of the Advanced Light Source is supported by the Director of the Office of Science, Office of Basic Energy Sciences, of the U.S. Department of Energy under Contract No. DE-AC02-05CH11231.

References

1. Knop K, Hoogenboom R, Fischer D, Schubert US. Angew Chem, Int Ed. 2010; 49:6288–6308.
2. Fruijtier-Poelloth C. Toxicology. 2005; 214:1–38. [PubMed: 16011869]
3. Greenwald RB, Choe YH, McGuire J, Conover CD. Adv Drug Delivery Rev. 2003; 55:217–250.
4. Alexandridis P, Alan Hatton T. Colloids Surf A. 1995; 96:1–46.
5. Olofsson K, Malkoch M, Hult A. RSC Adv. 2014; 4:30118–30128.
6. Santander-Borrego M, Green DW, Chirila TV, Whittaker AK, Blakey I. J Polym Sci, Polym Chem. 2014; 52:1781–1789.
7. Chiappetta DA, Sosnik A. Eur J Pharm Biopharm. 2007; 66:303–317. [PubMed: 17481869]
8. Kabanov AV, Lemieux P, Vinogradov S, Alakhov V. Adv Drug Delivery Rev. 2002; 54:223–233.
9. Weinand C, Pomerantseva I, Neville CM, Gupta R, Weinberg E, Madisch I, Shapiro F, Abukawa H, Troulis MJ, Vacanti JP. Bone. 2006; 38:555–563. [PubMed: 16376162]
10. Cortiella J, Nichols JE, Kojima K, Bonassar LJ, Dargon P, Roy AK, Vacant MP, Niles JA, Vacanti CA. Tissue Eng. 2006; 12:1213–1225. [PubMed: 16771635]

11. Schmolka IR. J Biomed Mater Res. 1972; 6:571–82. [PubMed: 4642986]
12. Nalbandian RM, Henry RL, Balko KW, Adams DV, Neuman NR. J Biomed Mater Res. 1987; 21:1135–48. [PubMed: 3667639]
13. Hunt JN, Feldman KE, Lynd NA, Deek J, Campos LM, Spruell JM, Hernandez BM, Kramer EJ, Hawker CJ. Adv Mater. 2011; 23:2327–2331. [PubMed: 21491513]
14. Yoon H, Dell EJ, Freyer JL, Campos LM, Jang WD. Polymer. 2014; 55:453–464.
15. Obermeier B, Wurm F, Mangold C, Frey H. Angew Chem, Int Ed Engl. 2011; 50:7988–97. [PubMed: 21751305]
16. Barthel MJ, Schacher FH, Schubert US. Polym Chem. 2014; 5:2647–2662.
17. Pounder RJ, Willcock H, Ieong NS, O'Reilly RK, Dove AP. Soft Matter. 2011; 7:10987–10993.
18. Yu Y, Gao Z, Zhan G, Li L, Li S, Gan W, Crivello JV. Chem – Eur J. 2007; 13:2920–2928. [PubMed: 17183596]
19. Pruitt, ME.; Baggett, JM.; to Dow Chemical Co. US Patent. 2,706,181. 1955.
20. Le Borgne A, Spassky N, Jun CL, Momtaz A. Makromol Chem. 1988; 189:637–50.
21. Takeda N, Inoue S. Makromol Chem. 1978; 179:1377–81.
22. Wu B, Harlan CJ, Lenz RW, Barron AR. Macromolecules. 1997; 30:316–318.
23. Vandenberg, EJ.; to Hercules Incorporated. US Patent. 3,219,591. 1965.
24. Yoshino N, Suzuki C, Kobayashi H, Tsuruta T. Makromol Chem. 1988; 189:1903–13.
25. Widger PCB, Ahmed SM, Coates GW. Macromolecules. 2011; 44:5666–5670.
26. Widger PCB, Ahmed SM, Hirahata W, Thomas RM, Lobkovsky EB, Coates GW. Chem Commun. 2010; 46:2935–2937.
27. Hirahata W, Thomas RM, Lobkovsky EB, Coates GW. J Am Chem Soc. 2008; 130:17658–17659. [PubMed: 19067512]
28. Peretti KL, Ajiro H, Cohen CT, Lobkovsky EB, Coates GW. J Am Chem Soc. 2005; 127:11566–11567. [PubMed: 16104709]
29. Balbo Block MA, Hecht S. Macromolecules. 2008; 41:3219–3227.
30. Price CC, Osgan M. J Am Chem Soc. 1956; 78:4787–92.
31. Schaus SE, Brandes BD, Larrow JF, Tokunaga M, Hansen KB, Gould AE, Furrow ME, Jacobsen EN. J Am Chem Soc. 2002; 124:1307–1315. [PubMed: 11841300]
32. Show K, Gupta P, Kumar P. Tetrahedron Asymmetry. 2011; 22:1212–1217.
33. Schilling FC, Tonelli AE. Macromolecules. 1986; 19:1337–43.
34. Carlotti S, Labbe A, Rejsek V, Doutaz S, Gervais M, Deffieux A. Macromolecules. 2008; 41:7058–7062.
35. Lundberg P, Lee BF, van den Berg SA, Pressly ED, Lee A, Hawker CJ, Lynd NA. ACS Macro Lett. 2012; 1:1240–1243. [PubMed: 23205320]
36. Ilavsky J. J Appl Crystallogr. 2012; 45:324–328.
37. Temple K, Kulbaba K, Power-Billard KN, Manners I, Leach KA, Xu T, Russell TP, Hawker CJ. Adv Mater. 2003; 15:297–300.
38. Ding J, Price C, Booth C. Eur Polym J. 1991; 27:891–4.
39. Ding J, Heatley F, Price C, Booth C. Eur Polym J. 1991; 27:895–9.
40. Chisholm MH, Navarro-Llobet D. Macromolecules. 2002; 35:2389–2392.
41. Ye HM, Xu J, Guo BH, Iwata T. Macromolecules. 2009; 42:694–701.
42. Li Y, Huang H, He T, Wang Z. ACS Macro Lett. 2012; 1:154–158.
43. Lotz B, Cheng SZD. Polymer. 2005; 46:577–610.
44. Zhu L, Cheng SZD, Calhoun BH, Ge Q, Quirk RP, Thomas EL, Hsiao BS, Yeh F, Lotz B. J Am Chem Soc. 2000; 122:5957–5967.
45. Hamley IW, Castelletto V. Prog Polym Sci. 2004; 29:909–948.
46. Bates FS. Macromolecules. 1985; 18:525–8.
47. Deplace F, Wang Z, Lynd NA, Hotta A, Rose JM, Hustad PD, Tian J, Ohtaki H, Coates GW, Shimizu F, Hirokane K, Yamada F, Shin YW, Rong L, Zhu J, Toki S, Hsiao BS, Fredrickson GH, Kramer EJ. J Polym Sci, Part B Polym Phys. 2010; 48:1428–1437.

48. Saville PM, Reynolds PA, White JW, Hawker CJ, Frechet JMJ, Wooley KL, Penfold J, Webster JRP. J Phys Chem. 1995; 99:8283–8289.

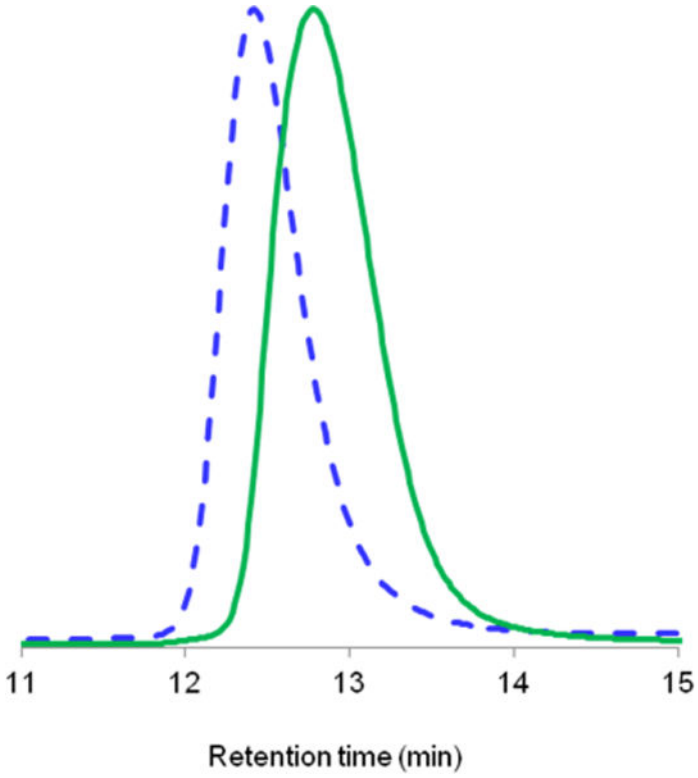

Figure 1.

GPC traces of PEO macroinititor (M_n = 20,000) ( ) and *it*-(*R*)-PPO-*b*-PEO-*b*-*it*-(*R*)-PPO (M_n = 28,800) after pollymerization of (*R*)-PO ( ).

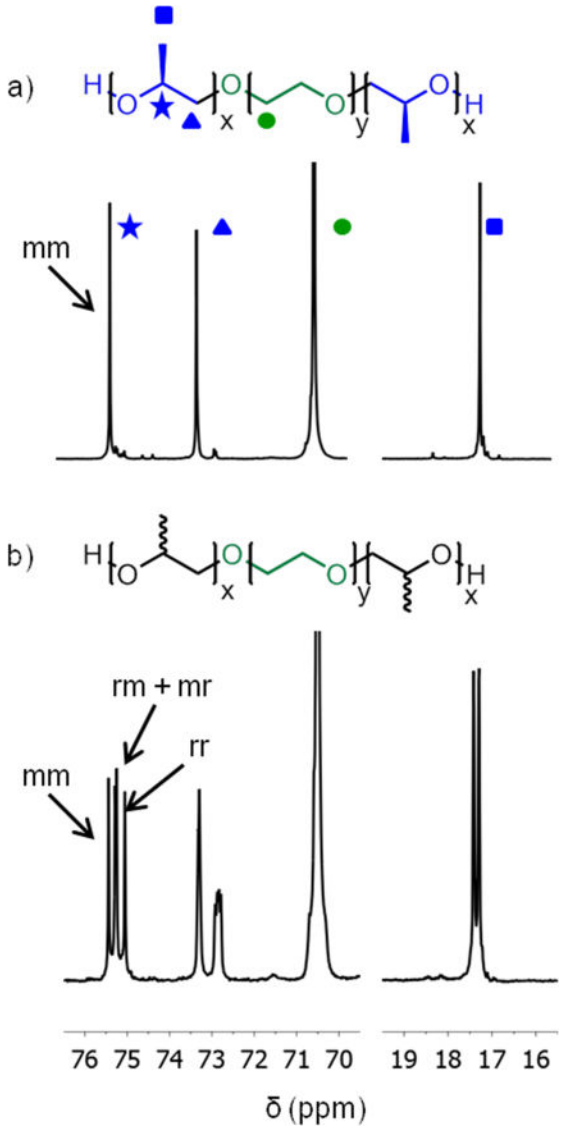

Figure 2.

^{13}C NMR spectra ($CDCl_3$, 150 MHz) of a) *it-(S)*-PPO-*b*-PEO-*b*-*it-(S)*-PPO, synthesized by polymerization of kinetically resolved PO from the PEO macroinitiator (M_n = 20,000), showing primarily *mm* triads and b) *at*-PPO-*b*-PEO-*b*-*at*-PPO, generated by polymerization of racemic PO from PEO macroinitiator (M_n = 20,000), showing a statistical distribution of *mm*, *rm*, *mr* and *rr* traids.

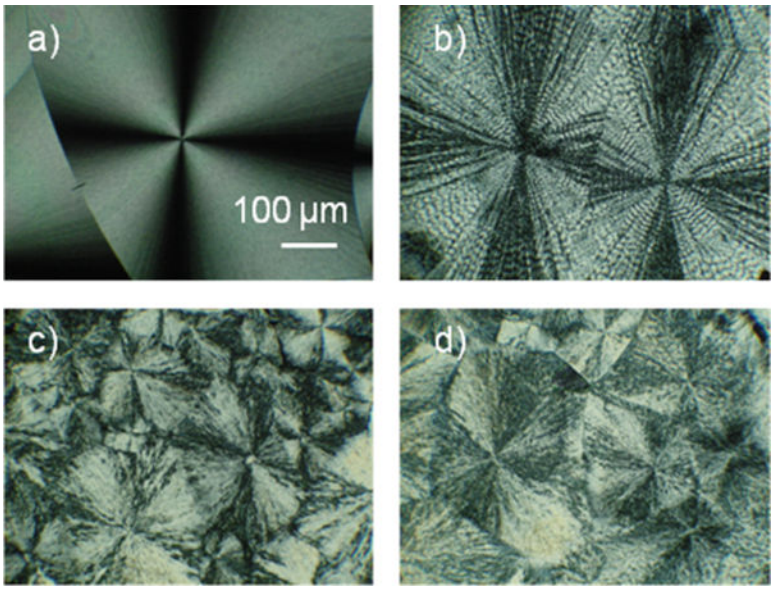

Figure 3.

Polarized optical micrographs of a) starting PEO homopolymer (M_n = 20,000 g/mol), b) control *it*-(*R*)-PPO homopolymer (M_n = 3,000 g/mol), c) *at*-PPO-*b*-PEO-*b*-*at*-PPO triblock copolymer (M_n = 28,600 g/mol) and d) *it*-(*R*)-PPO-*b*-PEO-*b*-*it*-*(R)*-PPO (M_n = 28,600 g/mol) triblock copolymer.

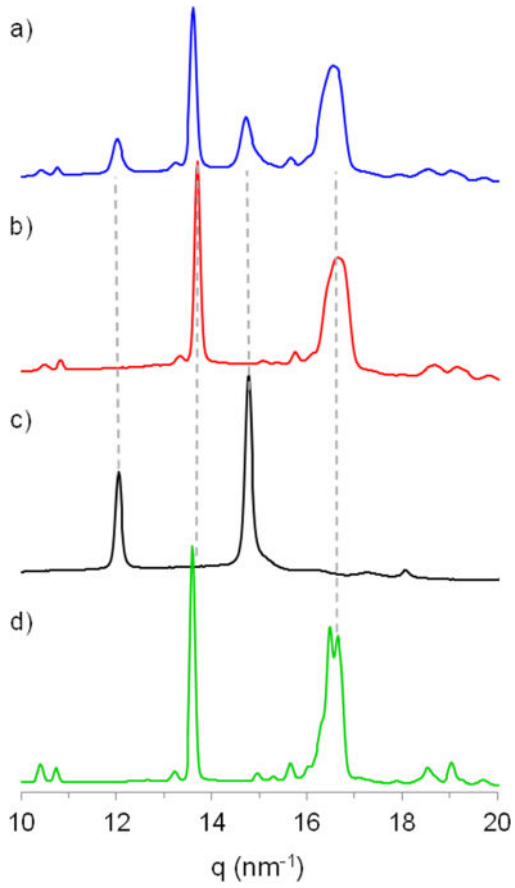

Figure 4.

WAXS profiles comparing a) *it*-(*R*)-PPO-*b*-PEO-*b*-*it*-(*R*)-PPO (⎯), b) *at*-PPO-*b*-PEO-*b*-*at*-PPO (⎯), c) *it*-PPO homopolymer (—) and d) starting PEO homopolymer (⎯), illustrating the presence of both *it*-(*R*)-PPO and PEO crystalline domains only in the *it*-PPO-*b*-PEO-*b*-*it*-PPO triblock sample.

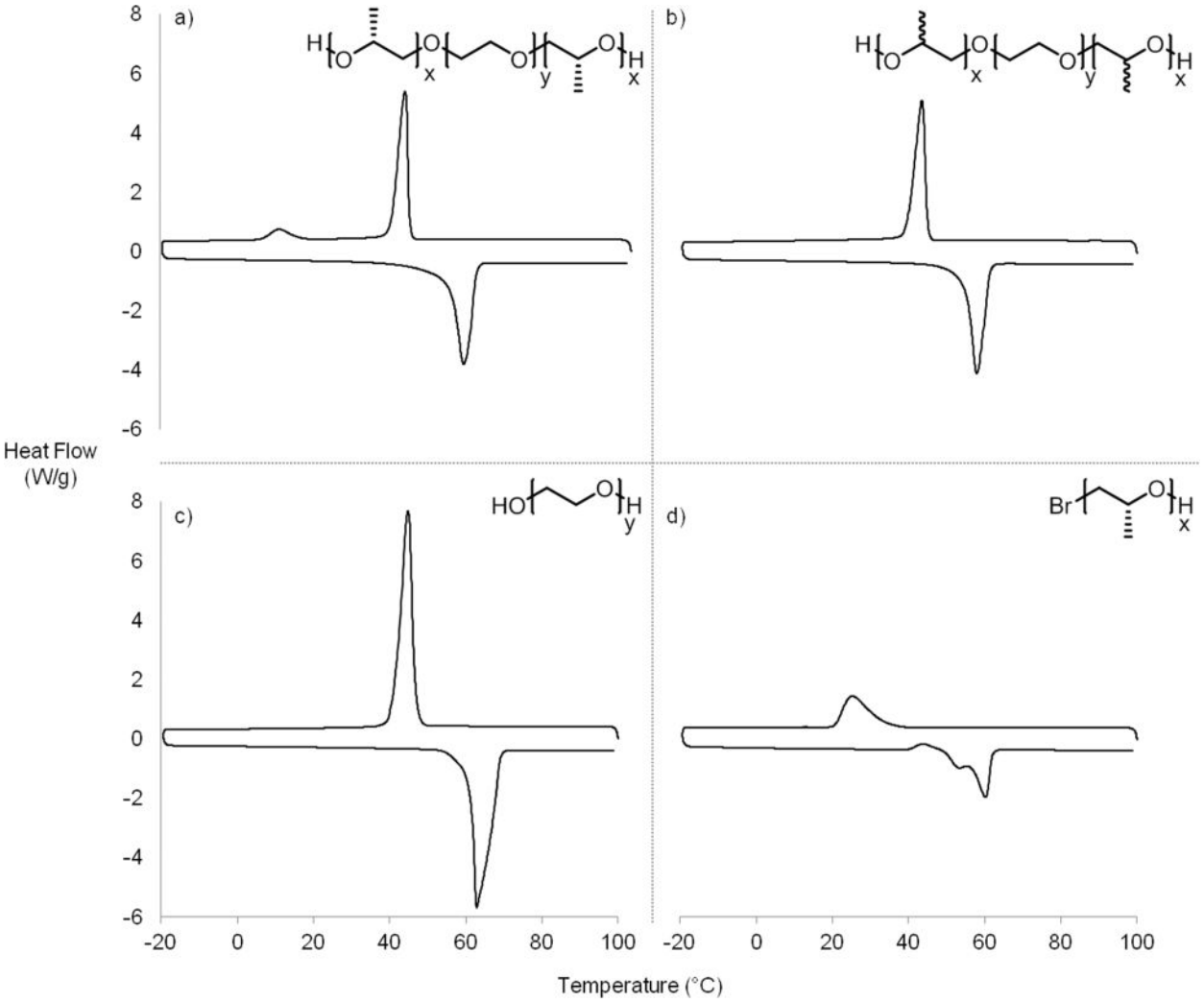

Figure 5.

DSC Thermograms for a) *it*-(*R*)-PPO-*b*-PEO-*b*-*it*-(*R*)-PPO, b) *at*-PPO-*b*-PEO-*b*-*at*-PPO, c) starting PEO homopolymer and d) *it*-(*R*)-PPO homopolymer. *it*-(*R*)-PPO-*b*-PEO-*b*-*it*-(*R*)-PPO has two distinct crystallization events, characteristic of double-semicrystalline domains.

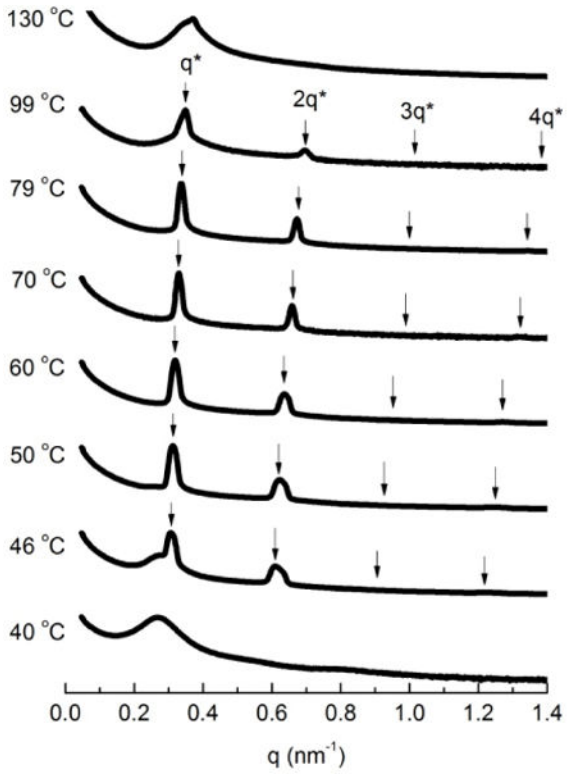

Figure 6.

Small angle x-ray scattering of *at*-PPO-*b*-PEO-*b*-*at*-PPO. Microphase separation occurs below 130 °C resulting in alternating PEO and PPO lamellae. PEO crystallization occurs below 46 °C, destroying the long range order and resulting in broad peaks. Arrows denote expected reflections for the lamellar morphology based on q*.

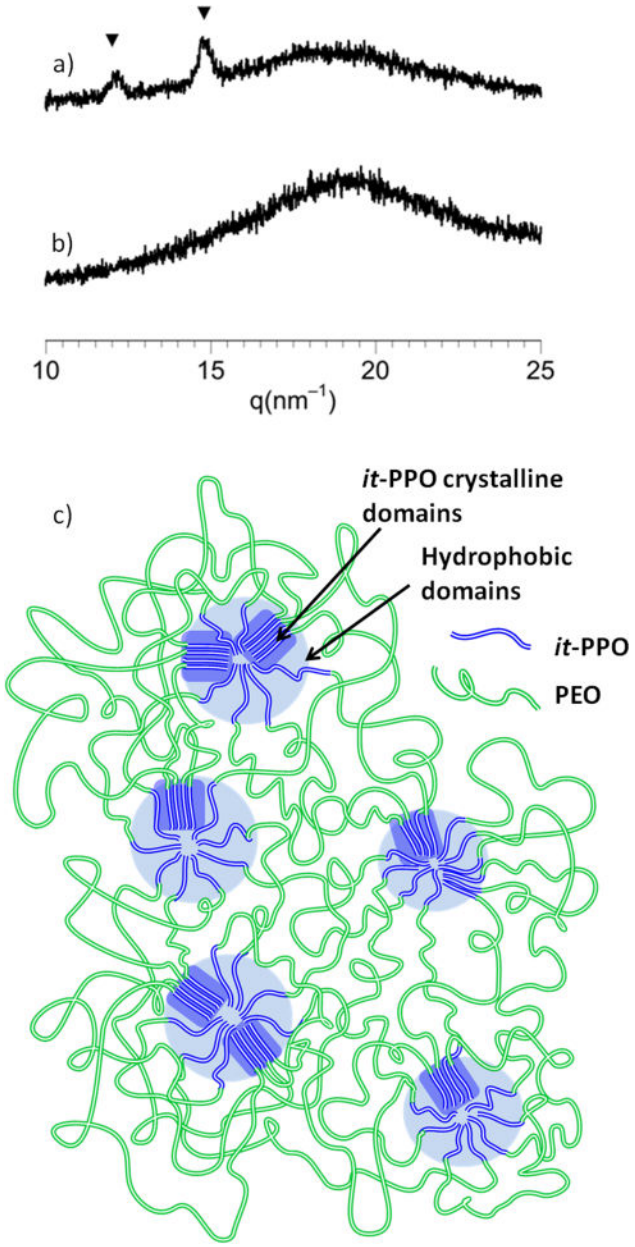

Figure 7.

Wide angle x-ray scattering of two hydrogels prepared by placing pressed films into water. (a) Reflections due to the presence of only *it*-(*S*)-PPO were present after hydrogel formation. Triangles indicate expected reflections for crystalline PPO. Low peak intensity is due to the limited number of scans we can obtain before the hydrogel starts to dry out. (b) No reflections were observed in the atactic triblock copolymer hydrogel. (c) Cartoon representation of hydrogel made of *iso*-PPO-*b*-PEO-*b*-*iso*-PPO showing the combination of hydrophobic interactions and crystalline crosslinks.

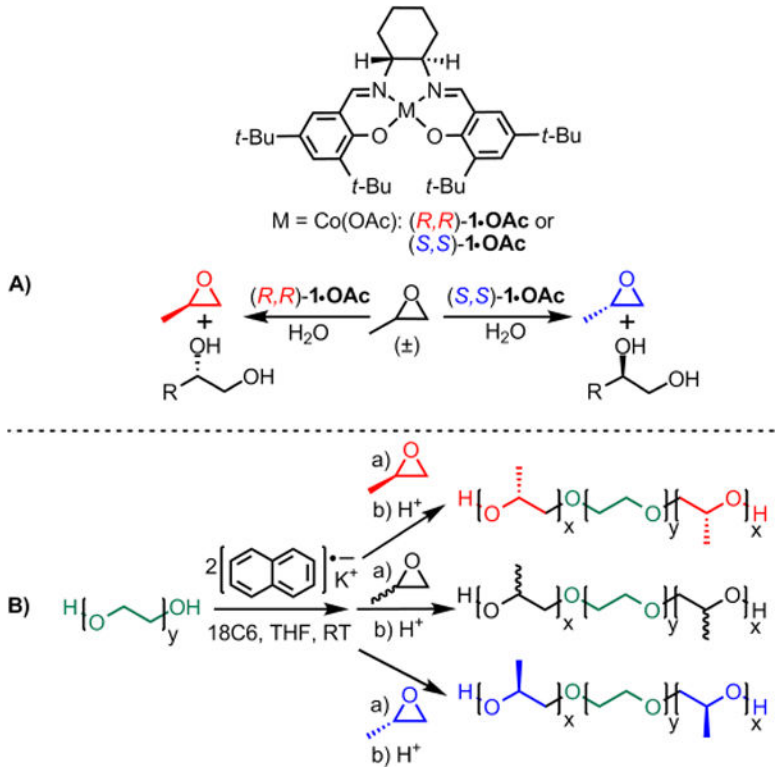

Scheme 1.

Methods for preparing PPO-*b*-PEO-*b*-PPO triblock copolymers: A) Hydrolytic kinetic resolution of PO using (salen)Co^{III}•OAc complex followed by B) Anionic ring-opening polymerization of kinetically resolved (*R*)- (top), (*S*)-(bottom) and racemic (middle) PO initiated from PEO alkoxide anions.

Table 1

Characterization of PPO-*b*-PEO-*b*-PPO triblock copolymers with various PPO end block lengths initiated from 10,000 or 20,000 g/mol[d] PEO macroinitiator.

No.	Monomer	M_n PEO	Đ PEO[a]	M_n PPO[b]	Đ PEP[a]	[*mm*] (%)[c]
1	(*S*)-PO	10000	1.11	4000	1.08	90
2	(*R*)-PO	10000	1.11	12000	1.17	90
3	(*R*)-PO	20000	1.30	8800	1.27	93
4	(*S*)-PO	20000	1.30	8600	1.26	90
5	(±)-PO	20000	1.30	8600	1.28	25

[a] Determined by GPC in chloroform, calibrated to PEO standards (g/mol), $Đ = M_W/M_n$.

[b] Total molecular weight of PO in the triblock copolymer determined by ^{1}H NMR spectroscopy.

[c] Content of *mm* triad in the triblock copolymer determined by ^{13}C NMR spectroscopy.

[d] See supporting information, S4 for further characterization of 20,000 g/mol PEO.